Electrically controlled topological micro cargo transportation
A. S. Bhadwal, N. J. Mottram, A. Saxena, I. C. Sage, and C. V. Brown
Supplementary Information File F1
Additional Experimental Details

Further information on Sec. 2.1 Device details and preparation

The device consisted of a layer of the nematic liquid crystal, E1, of thickness $d = 13$ μm sandwiched between two borosilicate glass substrates. The lower substrate at $z = 0$ was coated with a thin solid film which imparted low-pretilt planar nematic surface alignment. The opposing upper substrate at $z = d$ was coated with Teflon AF™ which imparted homeotropic nematic surface alignment.

The entire lower substrate was coated with a magnesium fluoride on zinc sulphide mechanical alignment layer with a combined thickness of 300 nm. A 120 nm zinc sulphide layer was thermally evaporated onto the substrate in vacuo (10^{-6} mbar) from pellets (CAS number 1314-98-3, Sigma-Aldrich / Merck KGaA, Darmstadt, Germany) heated in a tungsten basket. This layer acted as a passivation layer enabling crack free fabrication of the subsequent magnesium fluoride layer. A 180 nm magnesium fluoride layer was subsequently thermally evaporated onto the substrate in vacuo (10^{-6} mbar) from 3-6 mm pieces (CAS number 7783-40-6, Sigma-Aldrich / Merck KGaA, Darmstadt, Germany) heated in the tungsten basket. The magnesium fluoride layer was deposited with the plane of the substrate tilted at 45° to the evaporation direction to provide mechanical nano-groove planar alignment of the nematic liquid crystal.

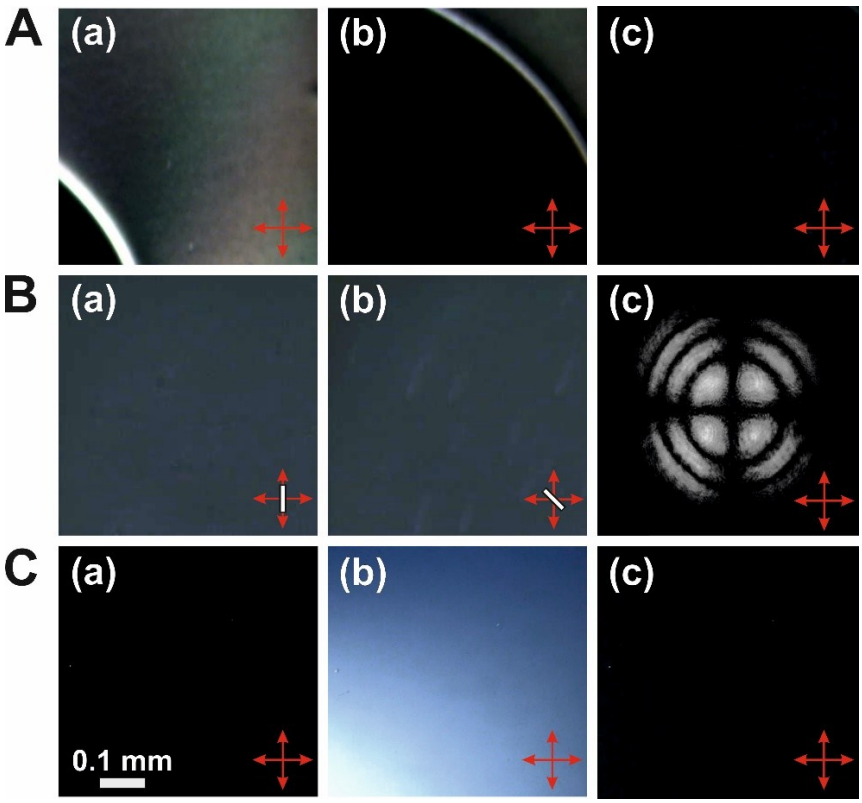

Fig. S1 Optical micrograph of a test cell containing a layer of the nematic liquid crystal material E1 and with Teflon AF™ coating on both internal surfaces that imparts homeotropic alignment. The micrograph images were taken using a 10× microscope objective under horizontal plane-polarised light with a crossed vertical analyser. (A) show images of the test cell immediately after capillary filling, in which the transient H-state is observed successively annealing out in the direction towards the top right corner. (B) (a) and (B) (b) show the fully annealed homeotropic state with the cell rotated at different orientations, (a) 0° and (b) 45°. (B) (c) shows a conoscopic image (a thicker cell was used in this image only), at a wavelength of 632.8 nm. (C) shows the optical texture in the cell before (a), during (b) and after (c) mechanical disruption achieved by tapping the cell.

For the homeotropic alignment layer on the top surface at $z = d$ a solution of Teflon AF ("PTFE AF 2400", Poly[4,5-difluoro-2,2-bis(trifluoromethyl)-1,3-dioxole-co-tetrafluoroethylene], dioxole 87 mol

%, CAS 37626-13-4, Sigma-Aldrich / Merck KGaA, Darmstadt, Germany), was made in its solvent, Octadecafluorodecahydronaphthalene (CAS numbers 37626-13-4 and 306-94-5, Sigma-Aldrich / Merck KGaA, Darmstadt, Germany), 0.75% by weight. The resulting solution was dip coated onto the substrate followed by drying at room temperature for 5 min and baking at 60°C for 10 min for removal of residual solvent.

The alignment of the nematic liquid crystal material E1 on our Teflon AF layer was tested by depositing the layer on glass coverslips, using the above process, and then creating a sandwich with a gap between the coverslips spaced by polyethylene terephthalate strips (PET, 13 µm, Goodfellow, Cambridge, UK). Hence for this test we used the same spacer thickness and spacer material as used in the assembly of the device in the micro cargo experiments, except that in the test cell both substrates were coated with the Teflon AF™ layer. Fig. S1 A shows different times immediately after capillary filling of the nematic material E1 into the test cell. In the top right of Fig. S1 A(a) the splay bend state, or "H-state" can be observed that is characteristic of nematic flow in the homeotropic geometry [e.g. see Physical Review E 80, 041706 (2009)]. This domain of the H-state grows out, Fig. S1 A (b), leaving a uniform homeotropic domain, Fig. S1 A(c), that appears dark between crossed polarisers. Fig. S1 B shows contrast enhanced images of the filled test cell at different orientations between crossed polarisers, with the test cell rotated 45° in the clockwise sense for the image in Fig. S1 B(b) compared to in Fig. S1 B(a). The very similar appearances and uniformity of the 2 images in Fig. S1 B (a) and Fig. S1 B(b) is consistent with the homeotropic aligned nematic layer exhibiting the expected zero birefringence. The image in Fig. S1 B (c) shows a conoscopic figure taken using uniform expanded illumination from a He-Ne laser at a wavelength of 632.8 nm, focused onto the cell with a 20× microscope objective, and with light collected using a 20× microscope objective that was also focused onto the cell. A cell with a larger 40 µm gap was used for Fig. S1 B (c) only in order to be able to observe a number of extinction rings. A uniaxial consocopic figure is obtained, as expected for a cell with homeotropic alignment. Fig. S1 C demonstrates the response of the nematic layer in the test cell to mechanical disruption caused by tapping the cell and monetarily decreasing the cell thickness. Fig. S1 C(a) shows the unperturbed layer, Fig. S1 C(b) shows the optical texture and expected increase in optical transmission during disruption, and Fig. S1 C(c) shows the recovered homeotropic texture immediately after the disruption.

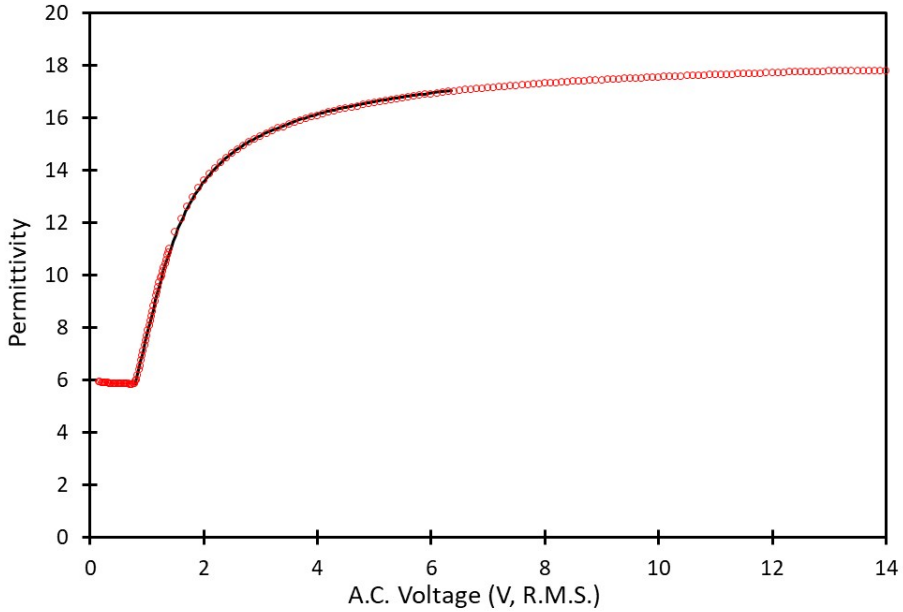

Fig. S2 A.C. voltage Fréedericksz transition curve for the nematic liquid crystal material, E1, which is a two component mixture of 5CB and 7CB in proportion 60% to 40% by weight. The material was contained within a commercial cell (Merck Chemicals Ltd.) with a cell gap of 22 µm. One surface of the cell had a continuous electrode whilst the other surface had a circular electrode with guard ring. The aligning agent on the cell surfaces was a rubbed PI polymer that gave a surface pretilt below 0.5° with a parallel configuration of the easy alignment axes on opposite surfaces. The open red circles show the permittivity measured at 21 °C as a function of an A.C. sinewave voltage (1 kHz) using an Impedance Analyser (Agilent 4284A). The solid black line shows a fit to the experimental data using nematic continuum theory.

To obtain dielectric and elastic physical parameters for the nematic material E1 the authors measured the A.C. voltage Fréedericksz transition curve for the same E1 formulation that was used in the experiments. We made the measurement in a commercial cell provided for this purpose by Merck Chemicals Ltd. and the resultant permittivity versus voltage curve is given in Fig. S2 (data is shown by red circles). Fitting nematic elastic continuum theory (solid black line above) to our measurement results provided the value of the positive dielectric anisotropy, $\Delta\varepsilon = 12.3 \pm 0.4$, and also the value of two of the elastic constants, the splay and bend elastic constants, $K_{11} = 7.2 \pm 0.5$ pN and $K_{33} = 10.1 \pm 0.8$ pN.

Further information on Sec. 3.1 Creation and electrical distortion of a topological defect line

In the main manuscript we note that the quality of fit between the theoretical model and the experimental results in the inset velocity versus voltage graph in Fig. 2 B deteriorates at higher voltages. Above 12 V the highly distorted regions localised around the defects embedded in the domain wall move closer to the substrates. Fig. S3 shows polarising optical micrographs of the high curvature tip of the electrically confined finger shaped domain at different voltages with two different points of focus of a 50× microscope objective. In Fig. S3 A the point of focus was close to the upper substrate near to the top of the layer, i.e. $z = d$, whilst in Fig. S3 B the vertical position of the device was moved closer to the objective to image through the layer so that the position of focus was close to the lower substrate, i.e. $z = 0$. The domain wall containing the disclination line can be seen in the images as the "C-shaped" cusp in the centre of the images with the cusp point towards the left hand side of the images. The images of the disclination lines with applied voltages of 10 V, 12 V and 15 V (R.M.S. amplitude of A.C. sinewave voltage at 1 kHz) are sharper when the point focus towards the top of the nematic layer (Fig. S3 A) compared to when the point of focus is towards the bottom of the nematic layer (Fig. S3 B). The images of the disclination line is in sharpest focus with an applied voltage of 15 V with the focus towards the top of the layer (Fig. S3 A), demonstrating that the disclination line moves towards the upper surface as the voltage is increased.

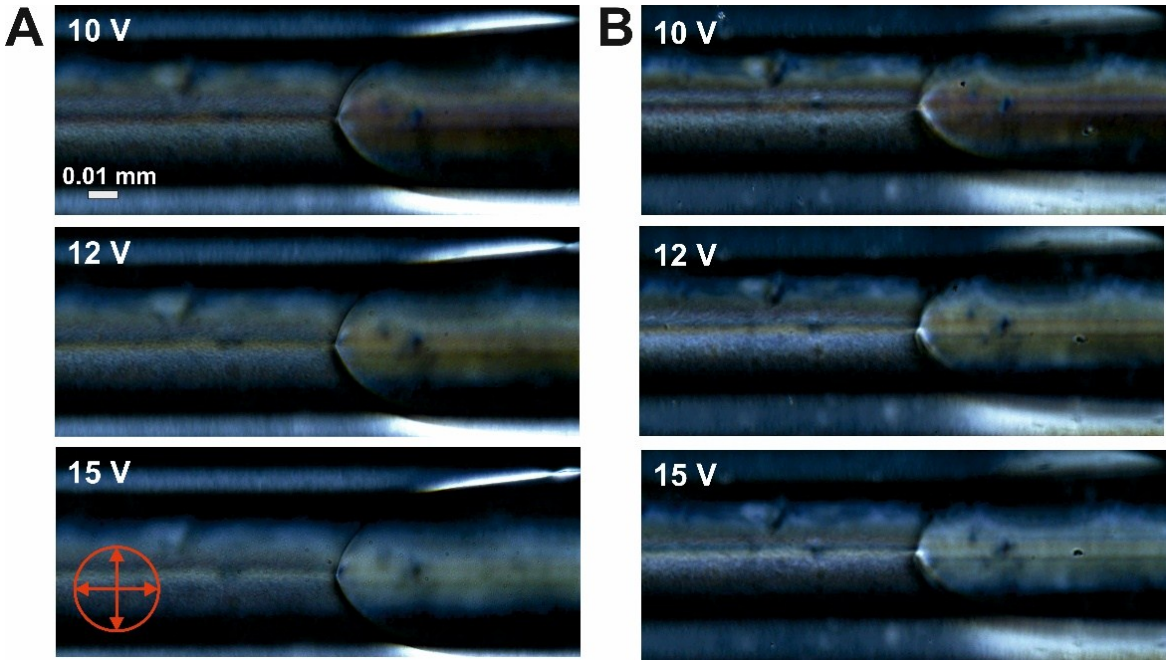

Fig. S3 Polarising optical micrographs of the high curvature tip of the electrically confined finger shaped domain at different applied voltages with two different points of focus of a 50× microscope objective. The device was orientated with the electrodes (along the x-direction) running horizontally. The nematic layer (thickness $d = 13$ μm) was examined in transmission under white light illumination between crossed polarisers with the polariser orientated horizontally and the analyser vertically. The images in (A) were taken with point of focus close to the upper substrate at the top of the layer, i.e. $z = d$, whilst in (B) the vertical position of the device was moved closer to the objective to image through the layer with the position of focus close to the lower substrate, i.e. $z = 0$. The x, y and z coordinates with respect to the layer are defined in Fig. 1 of the main manuscript.

Further information on Sec. 3.5 Electrically controlled topological micro cargo transportation

We have found that the colloidal particle typically stabilizes within the nematic layer, rather than being adhered at the wall. We estimated the positions of two different particles trapped near to the high curvature tip of an electrically confined finger shaped domains which were held stationary with an applied voltage equal to the critical stabilising voltage, V_C = 5.7 V. Fig. S4 shows polarising optical micrographs with three different points of focus of the 50× microscope objective. The images in Fig. S4 A and the images in Fig. S4 B are of different positions within the experimental device, with the positions of two different in-focus particles are indicated by the white arrows. In Fig. S4 A(a) and Fig. S4 B(a) the point of focus was close to the upper substrate near to the top of the layer, i.e. $z = d$, whilst in Fig. S4 A(c) and Fig. S4 B(c) the vertical position of the device was moved closer to the objective to image through the layer so that the position of focus was close to the lower substrate, i.e. $z = 0$. In Fig. S4 A(b) and Fig. S4 B(b) the vertical position of the device was moved to different points of focus that gave the sharpest images of the particles and that were intermediate between the upper and lower substrate focus points. From the positions of the microscope specimen stages at the different points of focus, we estimate that the centre line of the 5 μm diameter particles were between 4 μm and 5 μm above the lower substrate for the particle in Fig. S4 A, and between 9 μm and 10 μm above the lower substrate for the particle in Fig. S4 B.

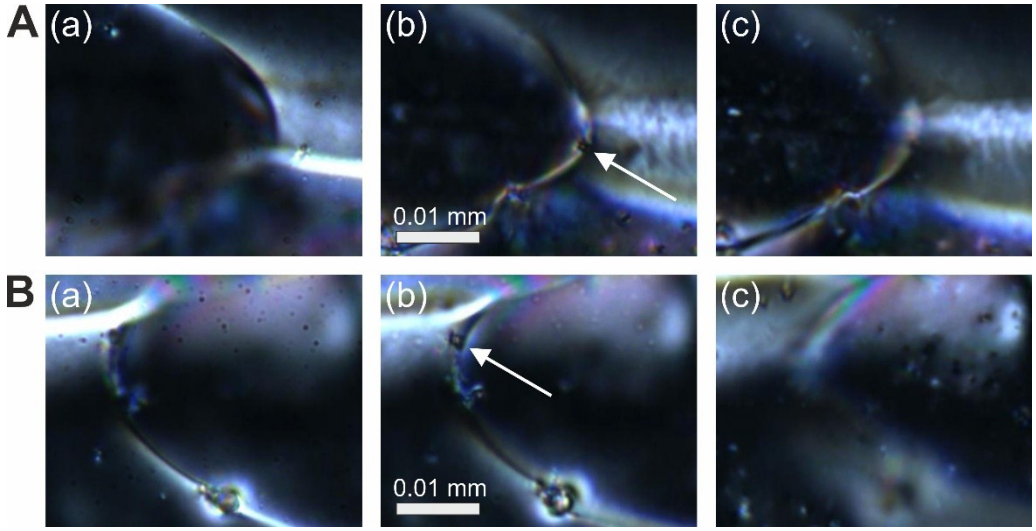

Fig. S4 Polarising optical micrographs of a colloidal particles trapped at the domain wall between two opposing HAN domains. The wall was held static by applying a voltage equal to the critical stabilising voltage, V_C = 5.7 V. The nematic layer (thickness d = 13 μm) was imaged using a 50× microscope objective in transmission under white light illumination between crossed polarisers with the polariser orientated horizontally and the analyser vertically. Images were taken at two different positions of the device at different ends of a finger shaped domain wall. The images (A)(a) and (B)(a) were taken with point of focus close to the upper substrate at the top of the layer, i.e. $z = d$. The vertical position of the device was moved closer to the objective to image through the layer, bringing the particle within the layer at intermediate focus in (A)(b) and (B)(b), and with the position of foci close to the lower substrate, i.e. $z = 0$, in (A)(c) and (B)(c).